Korean J. Chem. Eng., 35(2), 498-502 (2018)
DOI: 10.1007/s11814-017-0300-1

pISSN: 0256-1115
eISSN: 1975-7220

Improving the CO_2 fixation rate by increasing flow rate of the flue gas from microalgae in a raceway pond

Jun Cheng†, Zongbo Yang, Junhu Zhou, and Kefa Cen

State Key Laboratory of Clean Energy Utilization, Zhejiang University, Hangzhou 310027, China
(*Received 2 July 2016 • accepted 25 October 2017*)

Abstract−Residence time of flue gas bubbles with different solution velocities and the influence of NO_X and SO_2 from flue gas on pH values of culture solutions were analyzed based on large-scale raceway reactors. Microalgal growth and CO_2 fixation rates were also investigated with different gas flow rates. Bubble residence time was ~1.1 s when the solution velocity was 20 cm/s. The NO_X and SO_2 effects on microalgal growth were negligible, although 66% NO_X and 95% SO_2 were captured by the microalgal solution. Microalgal biomass productivity increased from 10.3 to 14.1 g/m^2/d when flue gas flow rate increased from 20 to 50 m^3/h. CO_2 fixation and microalgae biomass productivity increased further from 26.3 to 31.9 g/m^2/d and from 14.1 to 17.1 g/m^2/d, respectively, upon increase of flue gas flow rate from 50 to 150 m^3/h.

Keyword: CO_2 Fixation Rate, Raceway Reactor, Flue Gas

INTRODUCTION

Microalgal energy has been extensively researched in the contexts of CO_2 emission reduction and new energy development because microalgae undergo rapid growth and exhibit high utilization efficiency of sunlight energy. These microscopic plants are grown in large open ponds, into which power plant flue gas [1] or pure CO_2 (captured from power plants) is sparged, the biomass is converted to a fossil fuel replacement or preferably a high value liquid fuel such as biodiesel [2,3]. Furthermore, microalgal cultivation costs can be reduced when CO_2 from flue gas is efficiently used [4-6]. Large-scale CO_2 capture and utilization from power plants with microalgae cultivations can be an alternative process if the capital investments associated with carbon capture, transport and storage can be reduced or avoided [7]. Microalgal biomass production is only economically feasible when microalgae are considered not only a source of microalgal energy, but also the source of value-added bio-chemicals [8]. These processes, including biodiesel production [9] need to be optimized to attain feasibility. Raceway reactor is widely used because it is easy to operate and magnify [10,11].

Small indoor runway reactors have been used to investigate large raceway ponds [12-14]. Microalgal energy consumption and growth rate have also been studied [15,16]. Generation and rise trajectory of aeration bubbles were optimized with up-down chute baffles to improve CO_2 fixation rate with microalgae in raceway ponds [17]. Bubble generation process was measured with a high-speed photography system, which were affected by aerator orifice diameter, gas flow rate and paddlewheel speed. Bubble generation time decreased by 27% and bubble residence time increased by 27% with 10 r/min paddlewheel speed and 0.03 vvm aeration gas rate. In an algae raceway integrated design [18,19] culture system, several basins and canal are used to strengthen sunlight exposure and regulate temperature changes. Deepest daytime algal fluid is at 61 cm in this system, so a portion of algal liquid cannot capture light, resulting in low algal growth rate of approximately 3.47 g/m^2/d.

A channel raceway photobioreactor with a length of 100 m and width of 1 m was built by Mendoza et al. [20] to investigate effects of water depth, liquid velocity, and presence or absence of sump baffles in improving CO_2 supply transfer. Lowest specific power consumption was observed at a depth of 20 cm. Bubble generation and residence time were measured with a high-speed photography system [21]. Bubble generation times were all decreased because of the enhanced local solution velocity. Microalgae biomass yield increased by ~20% with shorter bubble generation time and longer bubble residence time in the raceway pond. Mass transfer coefficient and mixing time were measured with an online precise dissolved oxygen probes and pH probes system [22]. Mass transfer coefficient increased by 1.3-times and mixing time decreased by 33% when UCO baffles were used in the *H. pluvialis* solution, resulting in an 18% increase in biomass yield with 2% CO_2. However, different gas aerator arrangements with different gas flow rate were not analyzed. In an open raceway pond aerated with flue gas from a coal-fired power plant, CO_2 fixation between microalgal biomass and culture solution was compared with the weight ratio of biomass consumption at nighttime to biomass growth at daytime [23]. CO_2 fixation rate in the microalgal biomass increased from 18.4 to 40.7 g/m^2/d with an increase of average daytime sunlight intensity from 39,900 to 88,300 lux, which was approximately one-third of CO_2 removal rate from flue gas by the microalgal culture system. However, effects of gas flow rate on CO_2 fixation rate in microalgal biomass were not analyzed.

We analyzed bubble residence times with different solution veloc-

†To whom correspondence should be addressed.
E-mail: juncheng@zju.edu.cn
‡This paper is reported in the 11th China-Korea Clean Energy Workshop.

ities. Based on large-scale raceway reactors, NO_X and SO_2 influences from flue gas on pH value of culture solution were analyzed. CO_2 fixation rates and microalgal growth rates were also investigated with different gas flow rates.

MATERIALS AND METHODS

1. Materials

Microalgal strain used in the experiments was *Nannochloropsis oculata* obtained from Yantai Hairong Power Technology Company, Limited. Initial cultivation concentration of this strain was 0.1 to 0.2 g/L. Half of the culture solution was harvested every 2-4 days upon reaching a microalgal concentration of approximately 0.5 g/L. Flue gas from a coal-fired power plant was used with the following major components: 12±2% of CO_2, 120±10 ppm of NO_X, 50±10 ppm of SO_2. Sea water was used as basic culture solution with the following major metal ion components: 208,600 ppb of K^+, 6,877 ppb of Mg^{2+}, 630 ppb of Fe^{2+}, 160 ppb of Cu^{2+}, and 327 ppb of Zn^{2+}. To accelerate microalgal growth, 0.2 g/L of KNO_3, 0.045 g/L of Na_2HPO_4, and 0.005 g/L of $FeCl_3$ were added. Salinity was maintained at 32%±2% by adjusting fresh and sea water ratio.

2. Experimental Apparatus

The raceway pond culture system (Fig. 1) used to remove CO_2 from flue gas was the same pond as in the previous study [23]. Depth and volume of microalgal culture solution were 0.26 m and 310 m^3, respectively. Culture solution was moved by two paddlewheels. Raceway reactor contained five flue gas aeration zones. Each aeration area was 20-m-long and 5-m-wide and contained ten spargers. Flue gas was introduced to the raceway pond via gas pipeline system and equally allocated to five aeration zones.

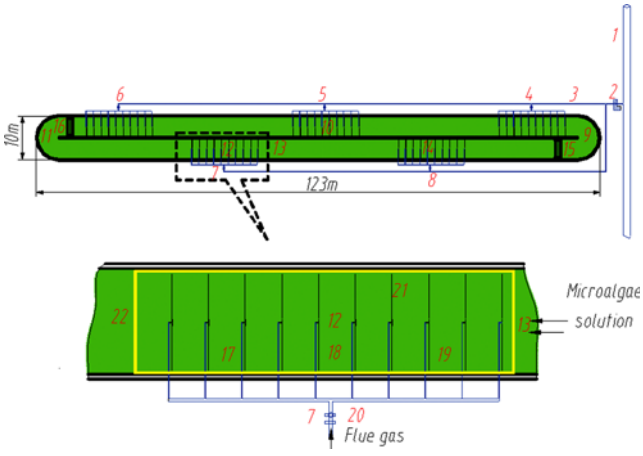

Fig. 1. Schematic of a 1,191 m^2 raceway reactor for microalgal growth and CO_2 fixation [23].
1. Transportation pipeline of flue gas with CO_2 concentration of 11.0-14.0% from coal-fired power plant to raceway reactor, 2. Forced draft fan, 3. Branch pipeline of flue gas, 4-8. Five aeration zones of flue gas with five flowmeters in the raceway reactor, 9-14. Six sampling points of microalgae solution, 15-16. Two paddle wheels, 17-19. Three sampling points of outlet gas from a sealed shed over microalgae solution for CO_2, SO_X and NO_X measurement, 20. Sampling point of inlet flue gas into the perspex-sealed shed over microalgae solution for CO_2 , SO_X and NO_X measurement measurement, 21. Rubber aerator of flue gas with ~0.7 mm pores, 22. Sealed shed over microalgae solution for CO_2 fixation measurement (yellow square shows cover area)

3. Test Procedures and Calculation

Sunlight intensity was determined by portable light meter (TES-1332A, Taiwan Taishi). Culture solution temperature and pH were measured with s portable pH meter (FG2, Mettler Toledo Switzerland); microalgal carbon element ratio was analyzed by using elemental analyzer (Flash EA1112, Thermo Finnigan). NO_X and SO_2 concentrations were measured with flue gas analyzer (MRU Vario Plus, Germany). In this study, sunlight intensity and culture solution temperature on the chart were average of values determined at four daily time points: 9:00, 11:00, 13:00, and 15:00.

3-1. Bubble Diameter and Velocity Measurement with High-speed Photography

Bubble generation process and movement were measured with the same method described by [24]. Sodium lamp was used as light source, and 1000 images were captured per second. Scale plates were added into raceway pond, so physical size of a pixel could be calculated with ArcGIS 9.3 and Microsoft Office Excel. With a time interval of 0.001 s between two adjacent images, average bubble diameter (D), average bubble horizontal velocity (V_x), and average bubble vertical velocity (V_y) could be calculated.

3-2. Growth and CO_2 Fixation Rate of the Microalgae

A total of six microalgal solution samples from the raceway pond were obtained (Fig. 1) twice daily at 7:00 and 18:00, so this 11 hours with sunlight was defined as one day during the calculation process. Each sample contained 60 mL of microalgal solution. Biomass was separated from medium by centrifugation at 7,000 rpm for 5 min in a high-speed desktop centrifuge (Heraeus Multifuge X1, Germany). Centrifugation was repeated thrice by adding deionized water to remove residual salt from microalgal biomass. Dry weight was determined after biomass was dried at 90 °C for 3 h. Microalgal biomass productivity (g/m^2/d) was calculated as follows:

$$m_{algae_j}=1/6\times\left(\sum_{i=1}^{6}b_i-\sum_{i=1}^{6}a_i\right)/d\times(V_{solution}\times10^3/S) \quad (1)$$

where m_{algae_j} is the microalgal biomass productivity on j day (g/m^2/d); a_i and b_i are biomass weights obtained from six sample points (9-14) at 7:00 and 18:00, respectively (g/L); S is the culture area of the large-scale raceway pond (1,191 m^2); and $V_{solution}$ is the algal solution volume (310 m^3).

Microalgal CO_2 fixation rate (g/m^2/d) was calculated as follows:

$$m_{CO_2algae_j}=m_{algae_j}\times\beta\times(44/12) \quad (2)$$

where $m_{CO_2algae_j}$ is the CO_2 fixation rate of microalgal biomass on j day (g/m^2/d), and β is the average ratio of carbon to microalgal biomass (0.51), β value was calculated based on the elemental analysis of the microalgal biomass powder obtained from the six microalgal solution samples at 18:00. Standard deviations of m_{algae_j} and $m_{CO_2algae_j}$ were calculated based on six independent point measurements. Standard deviations of growth and CO_2 fixation rate of the microalgae were calculated based on six independent measurements.

3-3. Measurement of the Inorganic Carbon (TIC) in the Medium

Total inorganic carbon (TIC) in the medium was determined

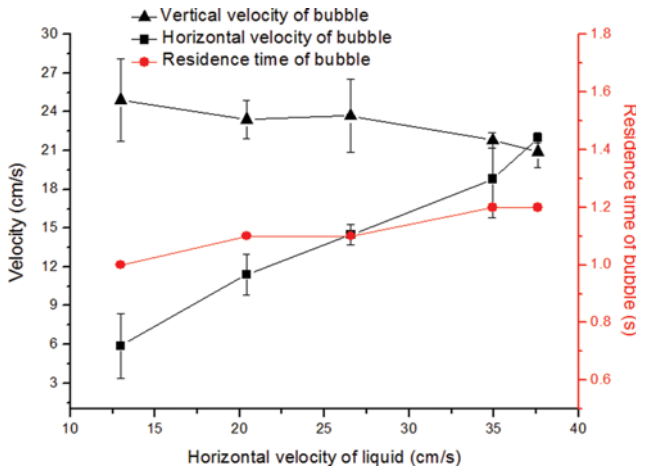

Fig. 2. Bubble residence time with different solution velocities.

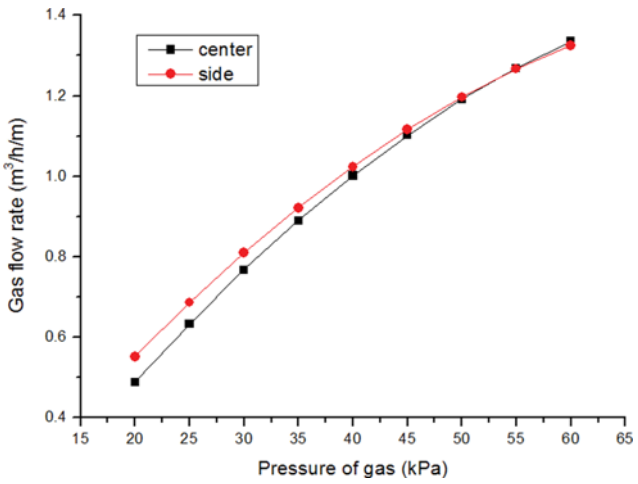

Fig. 3. Gas flow rate with different gas pressures.

by titration. A total of 20 mL standard $NaHCO_3$ solution (10 mmol/L) was placed in a small beaker and stirred with a magnetic stirrer. Afterward, 0.1 mol/L NaOH, 0.2 mol/L HCl, and 0.2 mol/L HCl were successively added to adjust pH to 9.0, 8.3, and 4.0, respectively; HCl volume used to regulate pH from 8.3 to 4.0 was marked V_1. Algal solution samples were evaluated using the same procedure, and HCl volume used in this case was marked V_2. The TIC concentration of the algal solution was calculated as follows: $TIC=10\times(V_2/V_1)$. Standard deviations of TIC concentration was calculated based on six independent measurements.

RESULTS AND DISCUSSION

1. Residence Times of Aeration Bubbles and Way of Flue Gas Aeration

Bubble residence time increased from 1.0 to 1.2 s (Fig. 2) and bubble diameter decreased from 1.7 to 1.5 mm, respectively, when solution velocity increased from 12.9 to 37.6 cm/s with an air aeration rate of 0.12 m^3/h. Bubble residence time was ~1.1 s when the solution velocity was 20 cm/s. Bubble residence time decreased further as gas flow rate increased. When orifice bubble was formed, the existing forces included inertia, drag, shear lift, and buoyancy [25]. Based on the effect exerted on the bubble, the forces can be divided into detaching and attaching forces. When the solution flowed horizontally, shear lift force had a leading influence on bubble removing from the aerator orifice [26]. With effects of horizontal velocity in the culture solution, shear lift and drag forces may lead to the detachment of early bubble. The production of small bubbles may be attributed to a large gas-solution interfacial area, as well as high mass transfer coefficient [27,28].

Gas flue rates were similar whether gas was introduced from one side of the 5-m-long gas aerator or from the center of the 5-m-long gas aerator. Gas flow rate increased from 0.5 to 1.3 m^3/h (Fig. 3) as gas pressure increased from 20 to 60 kPa. However, gas aeration was more uniform upon gas introduction from the center of the gas aerator. Flue gas flow rate was 0.6 m^3/h with fan outlet gas pressure at 34 kPa, and center gas pressure of the gas aerator at 25 kPa; therefore, pressure resistance of the gas pipeline system for the raceway pond microalgal culture system was ~9 kPa. Flue gas can be directly used in the microalgae culture industry with only volume flow rate control. There was about 500 m distance between the microalgae culture raceway pond and the power plant, so the temperature of flue gas decreased dramatically before it was introduced into the culture solution. Vapor in the flue gas became cooling water and discharged automatically during the culture process. On the other hand, the relative volume flow rate was only about 0.008 vvm as the largest volume flow rate of flue gas was 150 m^3/h.

2. Effects of NO_X, SO_2 from Flue Gas on pH Value of Microalgae Solution

The pH of the microalgal solution was affected by the acidity of NO_X and SO_2 in the flue gas. Culture solution pH decreased from 7.64±0.05 to 6.05±0.05 (Fig. 4) in the first hour upon introduction of flue gas at a flow rate of 150 m^3/h to the bottom of the raceway pond. The NO_X and SO_2 concentrations in the flue gas were 120±10 and 50±10 ppm, respectively. Microalgae solution pH decreased mainly due to increased HCO_3^- and H^+ ($CO_2+H_2O\rightarrow HCO_3^-+H^+$) concentrations before the medium was saturated. However, microal-

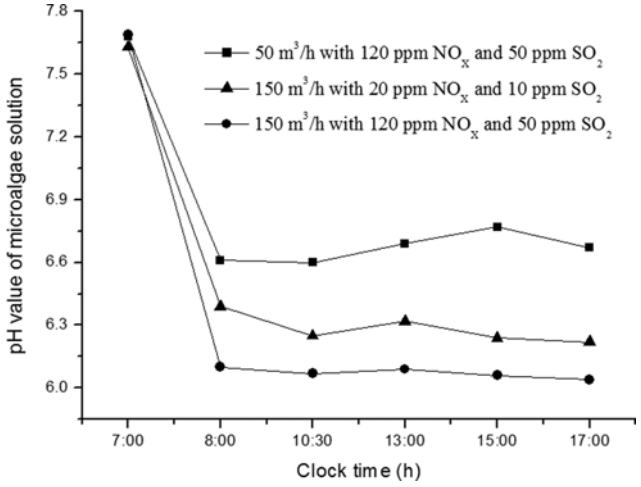

Fig. 4. Effects of NO_X and SO_2 from flue gas on pH value of microalgae solution.

gae solution pH increased from 6.05±0.05 to 6.30±0.15 when NO_X and SO_2 concentrations in the flue gas decreased from ~120 to ~20 ppm and ~50 to ~10 ppm, respectively. Gas composition of off-gas after treatment in the raceway pond was collected and measured. The concentration of NO_X and SO_X described was the values at several hours after inoculation, and approximately 55% CO_2, 66% NO_X and 95% SO_2 were scrubbed by the microalgal solution with gas flow rate of 150 m^3/h.

This work indicates the flue gas can be directly used in the microalgae culture industry only if the volume flow rate is controlled well, while the acidic gas in the flue gas like NO_X and SO_2 can be neglected. In the period of microalgal culture, without flue gas, culture solution pH would be over 10. Moreover, 50 kg/d $NaHCO_3$ was used as inorganic carbon source for microalgal growth. Acetic acid had to be used to control culture pH, as unstable pH values tend to allow growth of hybrid alga and pests in culture solution. The TIC concentration of the culture solution was 7±2 mmol/L during culture time with gas flow rate at 150 m^3/h. Therefore, the culture solution provided sufficient carbon to support microalgal growth [29].

3. Effects of Gas Flow Rate on CO_2 Fixation Rate in Microalgal Biomass

Mass transfer coefficient increases with increasing gas flow rate [30], resulting in accelerated CO_2 dissolution into culture solution. TIC concentration increased from 2.5±0.5 to 5±1 mmol/L upon increase of gas flow rate from 20 to 50 m^3/h. CO_2 fixation and microalgal biomass productivity increased from 19.2 to 26.3 g/m^2/d and from 10.3 to 14.1 g/m^2/d (Fig. 5), respectively. CO_2 fixation and microalgal biomass productivity increased further from 26.3 to 31.9 g/m^2/d and from 14.1 to 17.1 g/m^2/d (Fig. 5), respectively, upon increase of gas flow rate from 50 to 150 m^3/h. TIC concentration increased further from 5±1 to 7±2 mmol/L. To be used by microalgae, inorganic carbon sources generally were in the form of HCO_3^- which is transported into microalgae by transport proteins ($CO_2+H_2O \rightarrow HCO_3^-+H^+$; $HCO_3^-+H^+ \rightarrow CO_2+H_2O$). However, at high osmotic pressure (15% CO_2 of flue gas), CO_2 (not HCO_3^-) may transport directly through microalgal cell walls without transport proteins. At the photoreaction stage, it saved energy, and the Calvin cycle ($6CO_2+6H_2O \rightarrow C_6H_{12}O_6+6O_2$) was enhanced, as a result more CO_2 was captured. CO_2 fixation rate increased approximately 21% upon increase of gas flow rate from 50 to 150 m^3/h [31-33].

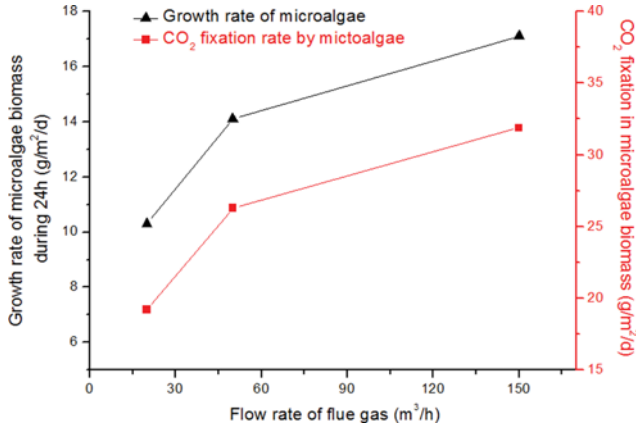

Fig. 5. Effects of gas flow rate on CO_2 fixation rate in microalgal biomass.

CO_2, ATP and NADPH were needed in the carbon fixation reaction stage (Calvin cycle). With flue gas aerated into the culture system, enough inorganic carbon could be offered (7±2 mmol/L). CO_2 transmission rate ($CO_2 \rightarrow HCO_3^- \rightarrow CO_2$) from culture solution into microalgal cells under high osmotic pressure condition and microalgal growth rate ($6CO_2+6H_2O \rightarrow C_6H_{12}O_6+6O_2$) increased significantly. Microalgal biomass productivity and CO_2 fixation rates were 18.5 and 34.6 g/m^2/d, respectively, with sunlight intensity of 75,400 lux and average solution temperature of 26.5±2.0 °C.

CONCLUSION

The NO_X and SO_2 effects on microalgal growth were negligible, although 66% NO_X and 95% SO_2 were captured by the microalgal solution. Microalgal biomass productivity and CO_2 fixation rates were 18.5 and 34.6 g/m^2/d, respectively, with flue gas flow rate of 150 m^3/h. Optimum flue gas flow rate based on different of sunlight intensities and solution temperatures should be studied in order to maximize CO_2 transfer efficiency, that is, minimize CO_2 losses for economic and environmental purposes.

ACKNOWLEDGEMENTS

This work was supported by National key research and development program-China (2016YFB0601003), National Natural Science Foundation - China (51476141), Zhejiang Provincial Natural Science Foundation - China (LR14E060002).

REFERENCES

1. K. Maeda, M. Owada, N. Kimura, K. Omata and I. Karube, *Fuel Energ. Abstracts*, **36**, 717 (1995).
2. J. R. Benemann, *Energ. Convers. Manag.*, **38**, S475 (1997).
3. J. R. Benemann, *Final Report to the US Department of Energy. National Energy Technology Laboratory Apcab* (2003).
4. I. Douskova, J. Doucha, K. Livansky, J. Machat, P. Novak, D. Umysova, V. Zachleder and M. Vitova, *Appl. Microbiol. Biot.*, **82**, 179 (2009).
5. C.-Y. Chen, K.-L. Yeh, R. Aisyah, D.-J. Lee and J.-S. Chang, *Bioresour. Technol.*, **102**, 71 (2011).
6. S. Y. Chiu, C. Y. Kao, T. T. Huang, C. J. Lin, S. C. Ong, C. D. Chen, J. S. Chang and C. S. Lin, *Bioresour. Technol.*, **102**, 9135 (2011).
7. S. Rezvani, N. R. Moheimani, and P. A. Bahri, *Comput. Chem. Eng.*, **84**, 290 (2016).
8. M. Šoštarič, D. Klinar, M. Bricelj, J. Golob, M. Berovič and B. Likozar, *New Biotechnol.*, **29**, 325 (2012).
9. B. Klofutar, J. Golob, B. Likozar, C. Klofutar, E. Žagar and I. Poljanšek, *Bioresour. Technol.*, **101**, 3333 (2010).
10. R. Harun, M. Singh, G. M. Forde and M. K. Danquah, *Renew. Sust. Energ. Rev.*, **14**, 1037 (2010).
11. N. R. Moheimani, *J. Appl. Phycol.*, **28**, 2139 (2015).
12. S. W. Li, S. J. Luo and R. B. Guo, *Bioresour. Technol.*, **136**, 267 (2013).
13. N. Moazami, A. Ashori, R. Ranjbar, M. Tangestani, R. Eghtesadi and A. S. Nejad, *Biomass Bioenergy*, **39**, 449 (2012).

14. P. E. Gharagozloo, J. L. Drewry, A. M. Collins, T. A. Dempster, C. Y. Choi and S. C. James, *J. Appl. Phycol.*, **26**, 2303 (2014).
15. D. Chiaramonti, M. Prussi, D. Casini, M. R. Tredici, L. Rodolfi, N. Bassi, G. Chini Zittelli and P. Bondioli, *Appl. Energy*, **102**, 101 (2013).
16. R. M. Handler, C. E. Canter, T. N. Kalnes, F. S. Lupton, O. Kholiqov, D. R. Shonnard and P. Blowers, *Algal Res. Biomass Biofuels Bioprod.*, **1**, 83 (2012).
17. J. Cheng, Z. Yang, Q. Ye, J. Zhou and K. Cen, *Bioresour. Technol.*, **201**, 174 (2016).
18. P. Waller, R. Ryan, M. Kacira and P. W. Li, *Biomass Bioenergy*, **46**, 702 (2012).
19. B. Crowe, S. Attalah, S. Agrawal, P. Waller, R. Ryan, J. Van Wagenen, A. Chavis, J. Kyndt, M. Kacira, K. L. Ogdenet and M. Huesemann, *Int. J. Chem. Eng.*, **2012**, 1 (2012).
20. J. L. Mendoza, M. R. Granados, I. de Godos, F. G. Acien, E. Molina, C. Banks *and S. Heaven*, *Biomass Bioenergy*, **54**, 267 (2013).
21. Z. Yang, J. Cheng, J. Liu, J. Zhou and K. Cen, *Bioresour. Technol.*, **216**, 267 (2016).
22. Z. Yang, J. Cheng, L. Ke, J. Zhou and K. Cen, *Bioresour. Technol.*, **214**, 276 (2016).
23. J. Cheng, Z. Yang, Y. Huang, L. Huang, L. Hu, D. Xu, J. Zhou and K. Cen, *Bioresour. Technol.*, **190**, 235 (2015).
24. Z. Yang, J. Cheng, R. Lin, J. Zhou and K. Cen, *Bioresour. Technol.*, **211**, 429 (2016).
25. C. J. Liu, B. Liang, S. W. Tang and E. Z. Min, *Chin. J. Chem. Eng.*, **21**, 1206 (2013).
26. K. Loubiere, V. Castaignede, G. Hebrard and M. Roustan, *Chem. Eng. Process.*, **43**, 717 (2004).
27. M. Ramezani, B. Kong, X. Gao, M. G. Olsen and R. D. Vigil, *Chem. Eng. J.*, **279**, 286 (2015).
28. K. Kim, J. Choi, Y. Ji, S. Park, H. Do, C. Hwang, B. Lee and W. Holzapfel, *Bioresour. Technol.*, **170**, 310 (2014).
29. E. Huertas, O. Montero and L. M. Lubián, *Aquacult. Eng.*, **22**, 181 (2000).
30. J. Cheng, Z. Yang, Q. Ye, J. Zhou and K. Cen, *Bioresour. Technol.*, **190**, 29 (2015).
31. J. A. Raven, *Photosynth. Res.*, **77**, 155 (2003).
32. Y. Matsuda, K. Nakajima and M. Tachibana, *Photosynth. Res.*, **109**, 191 (2011).
33. N. R. Moheimani and M. A. Borowitzka, *Appl. Microbiol. Biot.*, **90**, 1399 (2011).